UNIVERSIDADE FEDERAL DO MARANHÃO
CENTRO DE CIÊNCIAS EXATAS E TECNOLOGIA
Coordenação do Curso de Química Licenciatura e Bacharelado
Trabalho de Conclusão de Curso - TCC

GILVANA PEREIRA SIQUEIRA

ARRANJO DE MICROELETRODOS DE OURO NANOPOROSO USANDO MICROCHIPS: UMA PLATAFORMA ALTAMENTE SENSÍVEL E DE BAIXO CUSTO PARA APLICAÇÕES ELETROANALÍTICAS

SÃO LUÍS – MA
2022

GILVANA PEREIRA SIQUEIRA

ARRANJO DE MICROELETRODOS DE OURO NANOPOROSO USANDO MICROCHIPS: UMA PLATAFORMA ALTAMENTE SENSÍVEL E DE BAIXO CUSTO PARA APLICAÇÕES ELETROANALÍTICAS

Trabalho de Conclusão de Curso -TCC (em formato Artigo) apresentada junto à Coordenação do Curso de Química da Universidade Federal do Maranhão como um dos requisitos para obtenção do grau de Licenciada em Química.

Área de concentração: Química Analítica.

Orientadora: Profª. Dra. Luiza Maria Ferreira Dantas.

Coorientador: Prof. Dr. Iranaldo Santos da Silva.

SÃO LUÍS – MA
2022

Ficha gerada por meio do SIGAA/Biblioteca com dados fornecidos pelo(a) autor(a).
Diretoria Integrada de Bibliotecas/UFMA

Siqueira, Gilvana Pereira.
Arranjo de microeletrodos de ouro nanoporoso usando microchips : uma plataforma altamente sensível e de baixo custo para aplicações eletroanalíticas / Gilvana Pereira Siqueira. - 2022.
48 f.

Coorientador(a): Iranaldo Santos da Silva.
Orientador(a): Luiza Maria Ferreira Dantas.
Curso de Química, Universidade Federal do Maranhão, São Luís, 2022.

1. Dipyrone. 2. Electrochemical treatment surface. 3. Gold microelectrodes array. 4. Lead (II). 5. Microchips. I. Dantas, Luiza Maria Ferreira. II. da Silva, Iranaldo Santos. III. Título.

GILVANA PEREIRA SIQUEIRA

ARRANJO DE MICROELETRODOS DE OURO NANOPOROSO USANDO MICROCHIPS: UMA PLATAFORMA ALTAMENTE SENSÍVEL E DE BAIXO CUSTO PARA APLICAÇÕES ELETROANALÍTICAS

ESTA MONOGRAFIA FOI JULGADA ADEQUADA COMO UM DOS REQUISITOS OBRIGATÓRIOS PARA OBTENÇÃO DO GRAU DE **LICENCIADA EM QUÍMICA**

Aprovada em: 02/02/2022

BANCA EXAMINADORA:

_____

Orientadora: Profª. Dra. Luiza Maria Ferreira Dantas (UFMA)
Universidade Federal do Maranhão – UFMA

_____

1º Membro: Prof. Dr. Mauro Bertotti (IQ-USP)
Universidade de São Paulo - Instituto de Química – USP

_____

2º Membro: Profª. Dra. Rita de Cassia Silva Luz (UFMA)
Universidade Federal do Maranhão – UFMA

Dedico este trabalho aos meus pais Walter e Maria Girlene, e a Fátima Cordeiro a quem carinhosamente chamo de tia, que sempre me apoiaram a estudar e realizar meus sonhos, hoje mais um se tornou realidade, um sonho nosso!

AGRADECIMENTOS

São com lágrimas de gratidão e imensa felicidade que agradeço...

A Deus, por me dá força e sabedoria diante de cada dificuldade.

Aos meus pais Walter e Maria Girlene, por tudo nesta vida, pelo amor e incentivo nos estudos. E a minha madastra Sandra e sua família pelo carinho e ajuda recebida.

À minha tia Fátima, pelo abrigo, carinho, amor e por sempre acreditar que vou realizar meus sonhos. E a sua família, Cordeiro, por toda a ajuda e incentivo.

Ao meu namorado José Ribamar, por mim encorajar e ajudar nesses 4 anos de graduação; seu amor e carinho nos momentos mais difíceis foram essenciais para mim chegar até aqui.

À minha orientadora Profª. Dra. Luiza Maria Ferreira Dantas pela oportunidade de fazer iniciação científica, amizade, pelo conhecimento transmitido e por sempre acreditar no meu potencial e me incentivar todos dos dias.

Ao meu coorientador Profº. Dr. Iranaldo Santos da Silva, pelo conhecimento transmitido, amizade e ajuda no laboratório.

Aos professores do laboratório Auro Tanaka, Roberto, Marco e Ilanna, por todo suporte, momentos que me tiraram dúvidas e de companheirismo.

Aos meus amigos Matheus e João Pedro pela amizade, companheirismo, e ajuda nos estudos (principalmente por todas as madrugadas online respondendo questões e fazendo trabalhos), o nosso "grupinho" tem um lugar muito especial no meu coração.

A meu amigo José, pelo conhecimento transmitido durante seu mestrado, incentivo, ajuda e momentos de descontração, pois "não se dorme na Europa né?".

Aos meus amigos Anne, Mesaque, William e Jhonilson pelo acolhimento e suporte nos meus momentos iniciais no laboratório, amizade, e por todo incentivo na iniciação científica.

Às minhas amigas Thamires, Celiany e Maria Iraneide por serem o aconchego de uma amizade, pelos olhares de incentivo, conversas e risadas.

A todos os colegas e integrantes do Laboratório de Eletroquímica - LELQ, pelo acolhimento e momentos de descontração na "hora do dafé".

Aos professores, Rodrigo Alejandro Abarza Muñoz e Eduardo Mathias Richter, pelo suporte, acolhimento e orientação no Núcleo de Pesquisas em Eletroanalítica - NUPE, da Universidade Federal de Uberlândia – MG, durante meu intercâmbio nacional de pesquisa, e a todos os demais colegas do NUPE pelos três meses de grande aprendizado e companheirismo. E em especial, aos meus amigos Lucas ("BIA Men"), Raquel ("minha Raquelzinha"), David ("Printed Men") e Tiago ("Laser Men")

por toda ajuda, conhecimento que me foi ensinado, e risadas. Meus amigos nesses três meses no NUPE, nunca deu xabú! (devo mais 25 centavos pra você heim Tiago).

A minha amiga Mayane, por ter estado comigo nos últimos 3 meses de 2021, vivendo cada emoção no NUPE, pelas conversas, por ter me mostrado um outro lado de Deus por meio de pessoas muito especiais.

À Fundação de Amparo à Pesquisa e ao Desenvolvimento Científico e Tecnológico do Maranhão – FAPEMA, pela bolsa de Iniciação Científica concedida, a qual foi de grande ajuda para a realização deste trabalho.

À Coordenação de Aperfeiçoamento de Pessoal de Nível Superior – CAPES, pela bolsa concedida para realização do meu intercâmbio nacional de pesquisa, a qual foi essencial para realização do artigo a qual este trabalho se refere.

Ao Conselho Nacional de Desenvolvimento Científico e Tecnológico – CNPq, pelo fomento à pesquisa, e suporte financeiro vinculado a este trabalho.

E a Universidade Federal do Maranhão por desde o dia 12 de março de 2018 ter se tornado um segundo lar, e ter me ensinado que devemos estar preparados para o combate, e que a melhor preparação é o estudo.

Aos membros da banca examinadora, pelo aceite e por dedicarem seu tempo à leitura e avaliação deste trabalho, de forma a contribuir para seu aprimoramento e minha formação.

E a todos que me ajudaram e me ajudam, esta vitória é NOSSA!

MUITO OBRIGADA!

"O êxito da vida não se mede pelo caminho que você conquistou, mas sim pelas dificuldades que superou no caminho".

(Abraham Lincoln)

LISTA DE FIGURAS

LISTA DE TABELAS

LISTA DE ABREVIATURAS, SIGLAS E SÍMBOLOS

Au-µE – gold microelectrode array, em português, “arranjo de microeletrodos de ouro”

BIA-AD – bacht injection analysis coupled with amperometric detection, em português, análise por injeção em batelada com detecção amperométrica

BR – Britton Robinson buffer, em português, tampão Britton Robinson

CV – cyclic voltammetry, em português, voltametria cíclica

DIP – dipyrone, em português, dipirona

EDX – Energy Dispersive X-rays, em português, Energia Dispersiva por Raio-X

EIS – Electrochemical Impedance Spectroscopy, em português, Espectroscopia de Impedância eletroquímica

Ep – potential peak, em português, potencial de pico

f – frequency, em português, frequência

Ip – current peak, em português, corrente de pico

IUPAC – União Internacional de Química Pura e Aplicada

LELQ – Laboratório de Eletroquímica da UFMA

LOD – Limit of detection, em português, limite de detecção

LOQ – Limit of quantification, , em português, limite de quantificação

LSV –linear sweep voltametry, em português, voltametria de varredura linear

NPAu-µE–nonopous gold microelectrode array, em português, arranjo de microeletrodos de ouro nanoporoso

NPGFs – nanoporous gold films, em português, filmes de ouro nanoporoso

NUPE – Núcleo de Pesquisas em Eletroanalítica

R_{dis} – dispensing rate, em português, velocidade de dispensa

RSD – relative stantard deviations, em português, desvio padrão relativo

$R_{strirring}$ – strirring rate, em português, velocidade de agitação

SMD – Surface mounted device, em português, dispositivo de montagem em superfície

SWASV – square - wave anodic stripping voltametry, em português, voltametria de onda quadrada com redissolução anódica

V_{inj} – injection volume, em português, volume de injeção

a – amplitude

ΔE – step potential, em português, incremento de potencial

µEAs - microelectrode arrays, em português, arranjo de microeletrodos

µEs – microelectrodes, em português, microeletrodos

SUMÁRIO

ARTIGO / Manuscript

Nanoporous gold microelectrodes arrays using microchips: A highly sensitive and cost-effective platform for electroanalytical applications

Gilvana Pereira Siqueira[a,b], Lucas Vinícius de Faria[b], Raquel Gomes Rocha[b], Eduardo Mathias Richter[b], Rodrigo Alejandro Abarza Muñoz[b], Iranaldo Santos da Silva[a], Luiza Maria Ferreira Dantas[a**].*

[a]*Departamento de Tecnologia Química, Centro de Ciências Exatas e Tecnologia, Universidade Federal do Maranhão, 65080-805, São Luís, MA, Brasil*

[b]*Instituto de Química, Universidade Federal de Uberlândia, 38400-902, Uberlândia, Minas Gerais, Brasil*

Corresponding authors:

[*]*munoz@ufu.br* *ORCID: 0000-0001-8230-5825*

[**]*luiza.dantas@ufma.br* *ORCID: 0000-0002-2805-9253*

Abstract

In this paper, we investigate the effect of electrochemical treatment on the surface of low-cost and disposable devices (microchips) containing gold microelectrode arrays (Au-µE). This procedure involved the electrode anodization to generate nanoporous gold structures (NPAu-µE), which contributed to 4.4-fold increase in the electroactive area and decrease in the resistance to charge transfer. Energy-dispersive X-ray spectra revealed the formation of gold oxide nanostructures. The electrochemical response of these sensors was properly compared using dipyrone (DIP) and lead (II) as target species, and for both analytes, enhanced analytical performances were obtained under the treated surface (sensitivity increased from 3.3 to 6-times). A batch-injection analysis with amperometric detection was proposed for DIP that provided a detection limit of 0.57 µmol L^{-1}, precision of 4.0%, wide linear range (1.0–200.0 µmol L^{-1}), high analytical frequency (148 analyses per hour) and satisfactory application in pharmaceutical samples. Moreover, the NPAu-µE sensor proved to be suitable for Pb^{2+} evaluation by square-wave anodic stripping voltammetry, with an excellent analytical performance achieved, including a detection limit of 5.0 µg L^{-1} (24 nmol L^{-1}) linear range from 40.0 to 110.0 µg L^{-1}, and good precision (RSD = 4.3 %), which enabled the analysis of tap water samples.

Keywords: Microchips; Gold microelectrodes array; Gold nanoporous; Electrochemical treatment surface; Dipyrone; Lead (II).

1. Introduction

Gold based electrodes have been attractive material for their wide application in manufacture of electrochemical (bio)sensors, catalysis and energy conversion/storage systems[1]. Additionally, gold is one of the most used material for the production of microelectrodes (μEs)[1,2]. μEs, electrodes with dimension less than 100 μm (this at low scan rate) have some advantages over macroelectrodes, such as small size, high current density, improved mass-transport rate and reduced ohmic resistance in the electrochemical measurements, favoring the operation by a simple two-electrode system. This behavior is a result of the radial diffusion dominance, which generates a sigmoid voltammetric curve in the experiment. Nevertheless, μEs have a low faradaic current signal, which can limit the detection of many electrochemical species[3].

To overcome this problem, microelectrodes arrays (μEAs) have been regarded as promising alternative to a single μE, because they produce higher current intensity and keep the advantages of a single μE. In fact, in μEAs, each μE operates individually and contributes to the total measured current. Moreover, if the μEs are very close in the array, they act as macroelectrodes by reason of the adjacent diffusion zones can overlap/interact and improving the contribution of planar diffusion[1,2]. Further, the combination of their ultrasmall dimensions and electrochemical properties enables the monitoring chemical species in microenvironments (cells, neurons, etc.) in different science fields[3].

One of the commonest materials used in the fabrication of μEAs is gold. Generally, these electrodes are activated by polishing[4]; however, electrode surface renewal by this procedure can readily damage the thin layer and induce a heterogeneous surface. Currently, electrochemical activations were proposed in order to achieve a reproducible signal[5–8]. It has been reported that the activation generates nanoporous gold

films (NPGFs), providing a higher surface area and enhanced electroactivity properties when compared to gold electrodes which induce to a better electron transport.

The anodization of gold in oxalate solution to create nanoporous black film has been reported [5]; NPGFs have also been prepared using HCl medium[8] and reducing agent[9]. Jian *et al.* showed the As(III) detection using NPGFs prepared with $ZnCl_2$ in ionic-liquid medium[10]. The synthesis of NPGFs was proposed by dealloying of a silver/gold for the catalytic reduction of oxygen and hydrogen peroxide[11]. Even though these procedures are widely reported, the manipulation of dangerous chemicals and the long time required make these methods less feasible[4].

In this sense, Sukeri and collaborators[12] reported a green approach based on anodization followed by electrochemical reduction without the presence of binary alloys or reducing agents for the formation of NPGFs. Additionally, it was showed the electrocatalytic activity for dissolved oxygen reduction at a low overpotential, using NPGFs as working electrode. After that, the same group showed the application of the sensor for the determination of As(III) in acid medium using square-wave anodic stripping voltammetry (SWASV)[13].

Surface mounted device (SMD) is an important electronic device employed by technology industry due to simplicity, ultrasmall dimensions and higher mechanical resistance. Recently, some works have highlighted the development of low-cost sensors using SMD for detection of different analytes[7,14–17]. In this context, we propose the use of an SMD as a low-cost source of gold microelectrodes arrays and investigated the surface treatment effect on the electrochemical detection of organic and inorganic species. As proofs-of-concept, the SMD was assembled within a 3D-printed cell to perform the batch-injection analysis coupled with amperometric detection (BIA-AD) of dipyrone (DIP) and SWASV determination of lead(II).

2. Material and Methods

2.1 Reagents, Chemical, and Samples

All solutions were prepared using high purity deionized water with resistivity at least than 18 MΩ cm, obtained from a Milli Q water purification system (Millipore, Bedford, MA, USA). All reagents were of analytical grade and used without further purification. Sulfuric and acetic acids (98% w/v) were obtained from Vetec (Rio de Janeiro, Brazil). Analytical standard of DIP was obtained from Sigma-Aldrich (Darmstadt, Germany), phosphoric acid (85% w/v) and ferricyanide potassium were obtained from Labsynth (São Paulo, Brazil) and boric acid (99.8% w/w) was obtained from AppliChem Panreac (Barcelona, Spain).

The Britton-Robinson (BR) buffer (0.12 mol L^{-1}) was used as the supporting electrolyte for all electrochemical measurements involving DIP. This solution was composed of a mixture of 0.04 mol L^{-1} acetic, boric acid and phosphoric acids. The adjustment of pH values in the range of 2.0 to 9.0 was performed using NaOH solution (1.0 mol L^{-1}).

The standard solution of lead(II) was purchased from SpecSol (Brazil). Stock solutions of lead (II) were freshly prepared just before experiments by dilution in an appropriate supporting electrolyte (0.10 mol L^{-1} acetate buffer, pH = 4.5), as previous works described in the literature [18,19].

Pharmaceutical samples (tablets) were acquired in a local drugstore. In the sample preparation step, tablets were weighed and crushed to a fine and homogeneous powder. After that, 10 mg of this material was dissolved in the supporting electrolyte. Tap water samples were collected using plastic centrifuge tubes. These samples were spiked with 500.0 μg L^{-1} Pb^{2+}, diluted (10-fold) in supporting electrolyte and immediately analyzed.

2.2. Instrumentation and electrochemical measurements

All electrochemical measurements were performed using a μ-AUTOLAB type III or a PGSTAT 128 N potentiostat/galvanostat (Metrohm Autolab BV, Utrecht, the Netherlands) connected to a microcomputer, controlled by NOVA 2.1.4 software, at room temperature in the presence of dissolved oxygen.

For DIP analysis, a 3D-printed BIA electrochemical cell was used, as described by Cardoso *et al.*[20], employing acrylonitrile butadiene styrene (ABS) filament. This cell has a rounded cell cover in which are positioned the counter (platinum wire) and reference electrodes ($Ag|AgCl|KCl_{(sat.)}$) as well as the electronic micropipette (Multipette® Eppendorf stream) connected with a micropipette tip (Multipette® Combitip – 1mL). This system was placed in the cell in order to keep a distance of around 2 mm from the working electrode placed at the bottom of the cell in wall jet configuration. The micropipette has the key function in the BIA system that is the injection of DIP standard solutions or samples (precise and constant volumes and dispensing rates). A rubber O-ring was used to prevent leakage of the system making available all microelectrodes for electroanalysis. SWASV determination of Pb^{2+} was also accomplished using the 3D-printed electrochemical cell (internal volume of 10 mL) but without the micropipette required for BIA.

The elemental analysis of the electrode surfaces was carried out by Energy Dispersive X-rays (EDX) technique using an INCA X-Act (Oxford Instruments, Abingdon, UK) detector.

Electrochemical Impedance Spectroscopy (EIS) measurements were performed using the frequency range between 10 Hz to 50 kHz with signal amplitude of 10 mV, using to the 10.0 mmol L^{-1} $[Fe(CN)_6]^{4-/3-}$ redox reaction in the presence of 1.0 mol L^{-1} KCl solution, estimating impedance total (|Z|) through Bode plot.

2.3 Preparation of nanopourous gold microelectrode array platforms

The gold microelectrode arrays (Au-µE) were prepared from SMD microchips (Model:74HC244 990FW VW MYS 99 542, DigiKey Electronics®, Canada) which present gold microwires to connect the active part of the integrated circuit to the external terminals of a semiconductor[16,17].

Briefly, the fabrication of the Au-µE consists in the removal of the polymeric material from the top face of the microchip. For this, the device surface was successively polished using different sandpaper (400, 600 and 1500 grit, respectively), until the gold microwires were available. Figure S1 shows an image of the SMD chip (dimension 1.3 cm × 0.9 cm) used in this work, which contains an array composed of 20 gold microelectrodes. The cleaning of the Au-µE surface was performed by mechanical polishing with sandpaper (1500 Grit, 3M) moistened with deionized water, followed by successive washings. Afterwards, the device was fixed to a conductive plate (3.5 cm x 1.0 cm) with the aid of an adhesive tape and inserted in the electrochemical cell. Then, an electrochemical cleaning was performed using H_2SO_4 solution (0.50 mol L^{-1}) by cyclic voltammetry (CV) performing 15 successive scans in the potential range of 0.0 to +1.6 V with scan rate of 100 mV s^{-1}.

The nanoporous gold microelectrode array (NPAu-µE) was prepared in H_2SO_4 solution (0.50 mol L^{-1}) using a procedure described by Sukeri and colleagues [12], which consists of three electrochemical steps: (i) linear sweep voltammetry (LSV) with potential ranging of 0.0 to +2.0 V (*vs.* Ag|AgCl|$KCl_{(sat.)}$) and scan rate of 20 mV s^{-1}, (ii) constant potential aplieding of +2.0 V (*vs.* Ag|AgCl|$KCl_{(sat.)}$) for 600 s, and (iii) LSV with potential ranging of +2.0 to 0.0 V (*vs.* Ag|AgCl|$KCl_{(sat.)}$) and scan rate of 20 mV s^{-1}.

3. Results and discussion

3.1 Surface characterization of Au-µE and NPAu-µE

Gold based electrodes have been reported for the fabrication of electrochemical sensors towards many applications. To improve the electroactive area and sensitivity, various works explored different procedures to create nano or micro porous at the gold surface. Herein, the electrode was submitted to an electrochemical procedure to generated a nanopourous gold film according to a procedure reported by Sukeri *et al* [12] that demonstrated this protocol using a conventional gold disc-electrode.

Firstly, the surface of Au-µE and NPAu-µE were characterized by cyclic voltammograms in the potential range from 0.0 to +1.6 V in H_2SO_4 solution (0.50 mol L^{-1}) (Figure 1A). As can be seen, the peaks at +1.19 V (*vs.* Ag|AgCl|$KCl_{(sat.)}$) and +1.37 V (*vs.* Ag|AgCl|$KCl_{(sat.)}$) are attributed to the formation of gold oxides, and the reduction peak at +0.9 V (*vs.* Ag|AgCl|$KCl_{(sat.)}$) for NPAu-µE confirm the presence of gold structures on its surface as noticed by other authors in the formation of NPAu[12,13]. As expected, an improvement of the reduction current values of approximately 4.4-fold for NPAu-µE in relation to Au-µE was achieved. Moreover, the electroactive surface areas were estimated based on the gold oxide reduction peak, determined by integration, which is proportional to the real active surface area of the gold surface. The values obtained were 0.65 and 2.18 cm^2, for Au-µE and NPAu-µE, respectively (3.4-fold increase in electrochemical surface area).

According to the Bode plots, made by EIS measurements, shown in Figure S2, the impedances using NPAu-µE decrease substantially when compared to Au-µE. This behavior is attributed to the reduction of the double-layer impedance, induced by increase in the electrochemical surface area of the NPAu-µE[21]. Thus, due to their larger area, an electrocatalytic activity of the gold nanostructures is expected[12,22]. In order to confirm the

structural changes on the electrode surface, the elemental analysis of both surfaces was carried out by EDX (Figures 1B and 1C). According to the results, the formation of gold oxides in NPAu-µE is confirmed by the presence of elemental oxygen, even after gold reduction with linear sweep voltammetry.

It is important to highlight that the potential of +2.0 V (*vs.* Ag|AgCl|$KCl_{(sat.)}$) was chosen because at this region the oxygen evolution starts, thus suitable to create porous structures on the gold surface. According to Jaramarillo and collaborators[13], if more positive potentials are applied, more oxygen bubbles can be generated on the electrode surface which may affect the stability of the nanoporous film.

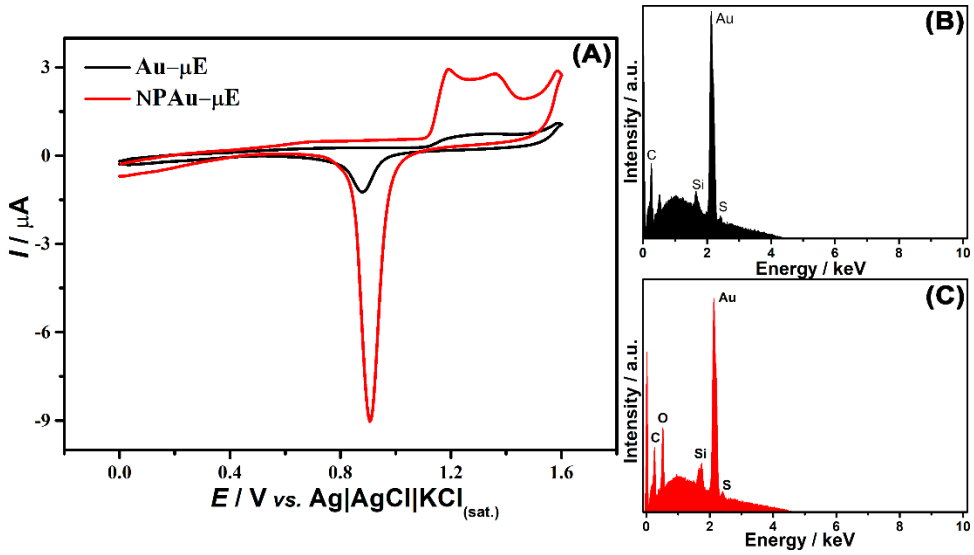

Figure 1. (A) Cyclic voltammograms of Au-µE (black line) and NPAu-µE (red line) in the supporting electrolyte 0.50 mol L^{-1} H_2SO_4 (scan rate: 100 mV s^{-1}; step potential: 5 mV). EDX spectra of **(B)** Au-µE and **(C)** NPAu-µE.

3.2 Electrochemical behavior of DIP using Au-µE and NPAu-µE

DIP was selected to be evaluated by Au-µE and NPAu-µE because it is one of the most consumed drugs in Brazil especially during the pandemic to treat fever caused by COVID-19. The electrochemical behavior of DIP was investigated on both electrodes by CV. For this, cyclic voltammograms were performed using DIP concentration (0.50 mmol

L^{-1}) in BR buffer (0.12 mol L^{-1}, pH 2.0), as shown in Figure 2. On the Au-µE, an oxidation signal with low intensity at around +0.57 V (*vs.* Ag|AgCl|$KCl_{(sat.)}$) was observed (Figure 2A), while on NPAu-µE, a well-defined signal at around +0.59 V (*vs.* Ag|AgCl|$KCl_{(sat.)}$) with an increase in current of 3.8-fold was verified. Probably, the improvement in the current response occurred by the porous gold nanostructures generated after the surface treatment. In this sense, NPAu-µE was selected for other studies involving DIP.

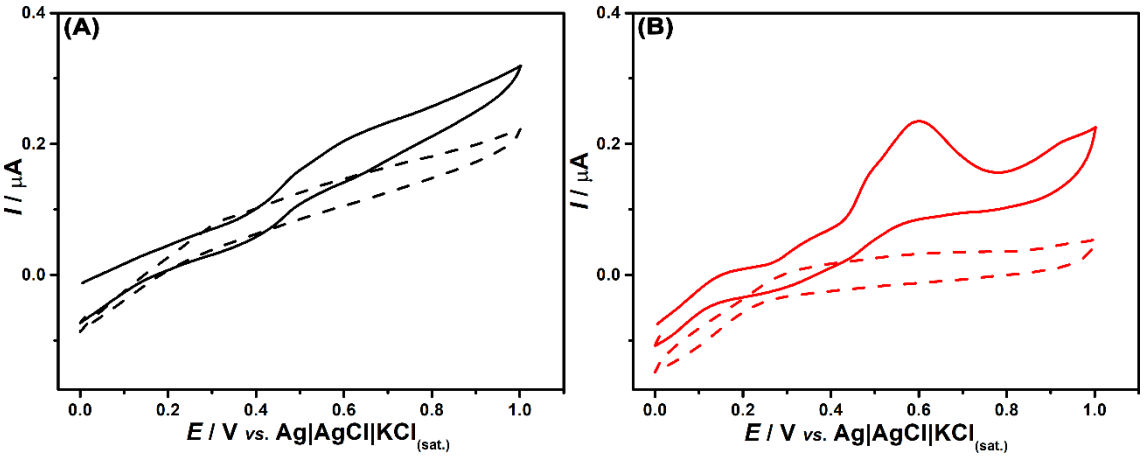

Figure 2. Cyclic voltammograms of 0.50 mmol L^{-1} DIP using **(A)** Au-µE and **(B)** NPAu-µE as working electrode The dashed lines refer the blank signals. The supporting electrolyte was BR buffer (0.12 mol L^{-1}; pH = 2.0). Scan rate: 50 mV s^{-1}, step potential: 5 mV.

Next, the pH influence on the electrochemical response of DIP (0.50 mmol L^{-1}) was evaluated using BR buffer solution (0.12 mol L^{-1}) with pH values in the range from 2.0 to 9.0 by LSV (Figure 3A). It can be seen in Figure 3B (Ep *vs.* pH) that the DIP oxidation process is pH-dependent, where a slope value (0.039 V pH^{-1}) suggests that in the DIP oxidation reaction involves a the one proton and two electron ratio which is in agreement with other works reported in the literature for DIP oxidation [23,24] .

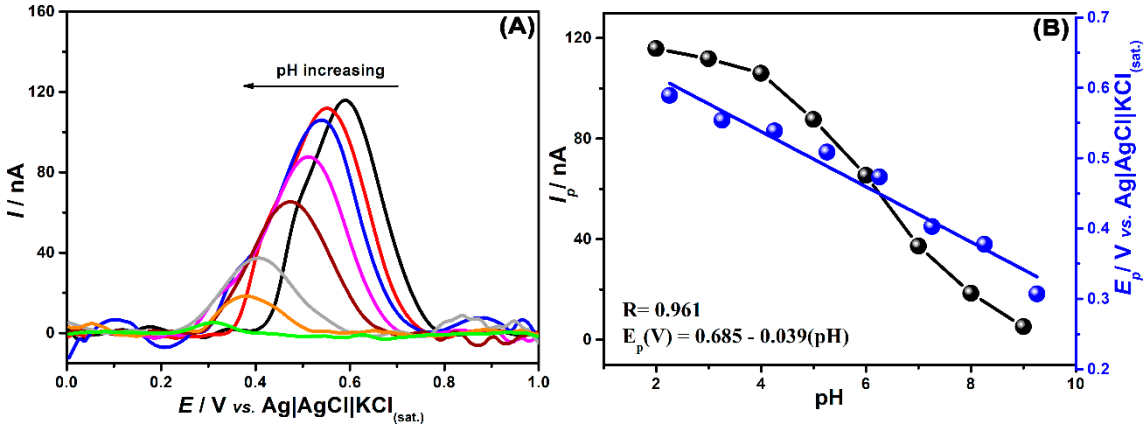

Figure 3. (A) Baseline-treated LSV response for 0.50 mmol L^{-1} DIP in 0.12 mol L^{-1} BR buffer solution (pH= 2.0 to 9.0) and **(B)** Correlation of current values (I_p) for different pH and potential peak values (E_p) using the NPAu-µE electrode. LSV conditions: scan rate of 50 mV s^{-1}; step potential of 5 mV.

It is worth highlighting that higher peak current value for DIP detection at NPAu-µE was achieved when 0.12 mol L^{-1} BR buffer solution (pH 2.0) was used. In order to obtain enhanced electrochemical results, 0.10 mol L^{-1} of HCl, $HClO_4$, and H_3PO_4 were also checked (Figure S3). However, better performance (peak shape and current intensity) was obtained with a 0.12 mol L^{-1} BR buffer (pH = 2.0) and, thus this solution was used in subsequent studies.

The investigation of the DIP oxidation process over NPAu-µE was also performed by CV using different scan rates (25-500 mV s^{-1}), in a BR buffer solution (0.12 mol L^{-1}, pH 2.0) and 0.50 mmol L^{-1} of DIP, as shown in Figure S4A. The plot data between the oxidation current versus square root of the scan rate (Figure S4B) showed a linear relationship (R = 0.999), indicating that its electro-oxidation process was predominantly controlled by diffusion of DIP species from the bulk to the NPAu-µE surface.

3.3 Determination of DIP by BIA-AD system

To evaluate the analytical performance of NPAu-µE for DIP quantification, the BIA-AD system was selected, as it provides adequate features for routine analysis, such as high analytical frequency, lower consumption of reagents and samples, and portability [25]. In order to obtain better sensitivity, precision and selectivity, some parameters related to BIA-AD, such as the applied potential (+0.3 to +1.0 V), injection volume (V_{inj} ,50 to 300 µL) and dispensing rate (R_{dis}, 17 to 299 µL s^{-1}), were carefully investigated. In these studies, all measurements were performed in triplicate (n = 3) using 50.0 µmol L^{-1} DIP. The influence of each parameter on the electrochemical response of the DIP is shown in Figure S5, and the optimized values are described in Table S1.

Under the selected parameters, analytical curves were prepared with increasing and decreasing DIP concentrations in the range from 1.0 to 200.0 µmol L^{-1} to investigate linear range and memory effect after successive injections of DIP standard solutions (Figure 4A). Correlation coefficient values (0.999 and 0.998) in ascending and descending concentration orders demonstrate good linearity, while similar slopes (0.962 and 0.965 μmol^{-1} L nA) indicate absence of memory effect on NPAu-µE surface. The same evaluation was carried out using Au-µE as working electrode, where a linear range of 5.0 to 200.0 µmol L^{-1} was obtained, as shown in supplementary material (Figure S6).

The limit of detection (LOD) was calculated according to International Union of Pure and Applied Chemistry (IUPAC), where LOD = 3.3sB/S (sB is the standard deviation of the intercept and S is the slope of the calibration curve). The calculated values were 5.0 and 0.57 µmol L^{-1} using untreated (Au-µE) and treated (NPAu-µE) surfaces, respectively. Figure 4B shows the data of analytical curves using both sensors, and it is possible to note that over NPAu-µE a greater sensitivity was achieved, due to the larger

active area. In fact, better figures of merit (LOD, linear range and sensitivity) were observed using NPAu-µE. These results agree with the preliminary observations by CV.

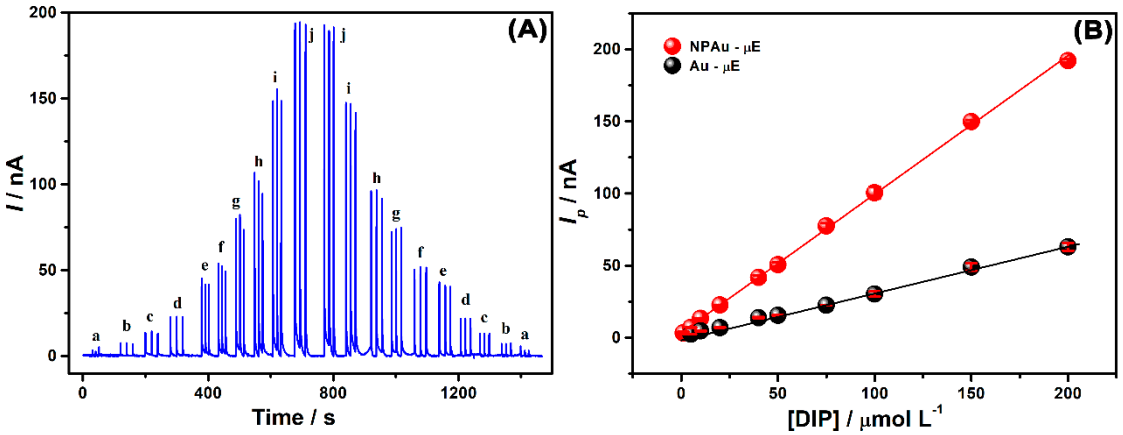

Figure 4. (A) Baseline-corrected amperograms of successive injections (n = 3) of DIP standard solution (a-j: 1.0 to 200.0 µmol L^{-1}) in increasing and decreasing concentrations, using the NPAu-µE as working electrode, and **(B)** Comparison between calibration curves of DIP in the NPAu-µE (red line) and Au-µE (black line). BIA-AD conditions: Applied potential = +0.7 V; supporting electrolyte: 0.12 mol L^{-1} BR buffer (pH = 2.0); V_{inj} = 200 µL, R_{dis} = 227 µL s^{-1}.

In order to assess the precision of the method using NPAu-µE, a repeatability study (n = 15) was performed for two concentration levels (50.0 and 100.0 µmol L^{-1}) (see Figure S7). The relative standard deviations (RSD) were 3.6 and 3.9% for low and high levels, respectively, which attested a good precision and stability of the nanoporous film. The analytical frequency was estimated as 148 analyses per hour. Table 1 summarizes the analytical features obtained for the determination of DIP using both sensors by BIA-AD system.

Table 1. Analytical features obtained for DIP using Au-µE and NPAu-µE sensors by BIA-AD system.

Analytical Parameters	Au-µE	NPAu-µE
Linear range / µmol L^{-1}	5.0 – 200.0	1.0 – 200.0
R	0.999*/0.998**	0.999*/0.998**
Intercept / nA	1.04*/1.93**	3.36*/2.34**
Slope / µmol $^{-1}$ L nA	0.290*/0.286**	0.962*/0.965**
LOD / µmol L^{-1}	5.00	0.57
RSD (n = 15; 50.0 and 100.0 µmol L^{-1}) /%	-	3.6#/3.9##

Injection in *ascending and **descending concentration order; # 50 µmol L^{-1} and ## 100 µmol L^{-1} of DIP.

Subsequently, the developed method was applied to determine DIP in two pharmaceutical formulations, as shown in Figure 5. Addition and recovery studies were carried out using 50.0 µmol L^{-1} DIP, and recovery values of 87±4 and 101±2 %, indicated the absence of matrix effect, as well as an adequate accuracy of the analyses. The DIP contents found in the samples (A and B) were 495±18 and 494±4 mg, respectively, which were in agreement with the value provided by manufacturers' labels (500 mg). Moreover, no memory effect was observed even after the addition of pharmaceutical samples, as can be seen in the Figure 5B.

The analytical performance of the proposed method for the determination of DIP was compared with other electroanalytical methods reported in the literature, as described in Table S2. It can be highlighted that the detectability of the NPAu-µE sensors was similar or better to more expensive electrochemical sensors (glassy carbon and platinum electrode) and a wide linear range. Furthermore, although not mentioned in Table S2, the BIA-AD method allowed extremely fast analysis, which is essential for routine applications in pharmaceuticals.

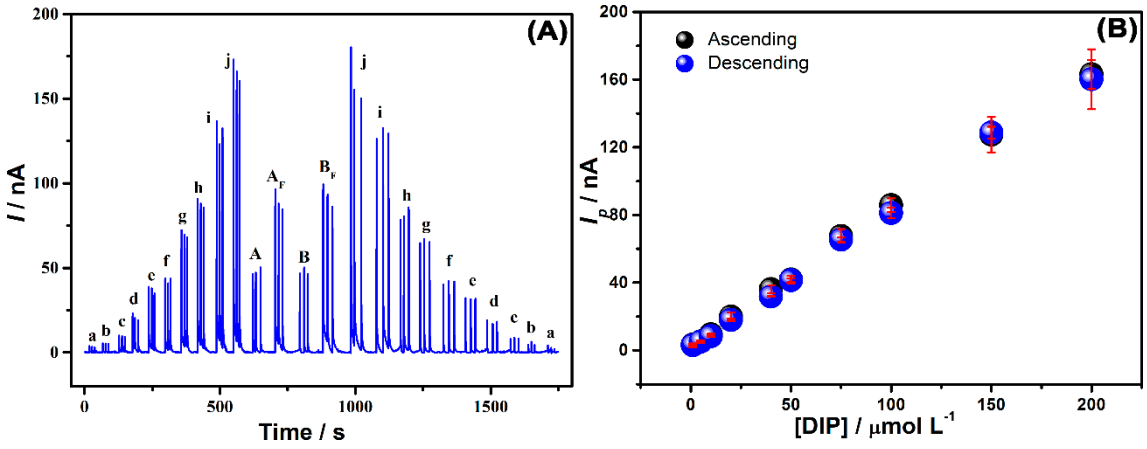

Figure 5. (A) Baseline-corrected amperogram of DIP standard solutions (a-j: 1.0 to 200.0 µmol L^{-1}), and pharmaceutical samples solutions (A and B samples) and spiked samples (A_F and B_F). **(B)** Calibration curves in the increasing and decreasing direction of concentration for DIP standard solutions (The decreasing curve was obtained after injection of samples). BIA-AD conditions: Applied potential = +0.7 V; supporting electrolyte: 0.12 mol L^{-1} BR buffer (pH 2.0); V_{inj} = 200 µL, R_{dis} = 227.3 µL s^{-1}.

3.4 Voltammetric determination of lead (II) by SWASV

The analytical performance of the proposed sensor was also investigated for the determination of inorganic species, Pb^{2+} ions, which is a highly toxic metal with great environmental monitoring relevance. For this, the SWASV technique was selected due to its greater sensitivity due to the electrochemical deposition step. The SWASV parameters (deposition time and potential, amplitude, step potential and frequency) and stirring rate were properly evaluated, and selected based on the higher analytical signal, precision and peak shape. Figures S8 to S13 present the studies involving each of the evaluated parameters mentioned above, using 50.0 µg L^{-1} Pb^{2+} and 0.10 mol L^{-1} acetate buffer pH 4.5 as the supporting electrolyte[19]. Table S3 summarizes the selected optimized values. Using these conditions, the electrochemical response of Pb^{2+} was checked using both sensors (Figure 6). It can be seen in the voltammograms that the current using NPAu-µE

was approximately 6-fold greater when compared with Au-µE. Thus, NPAu-µE was employed to Pb^{2+} detection.

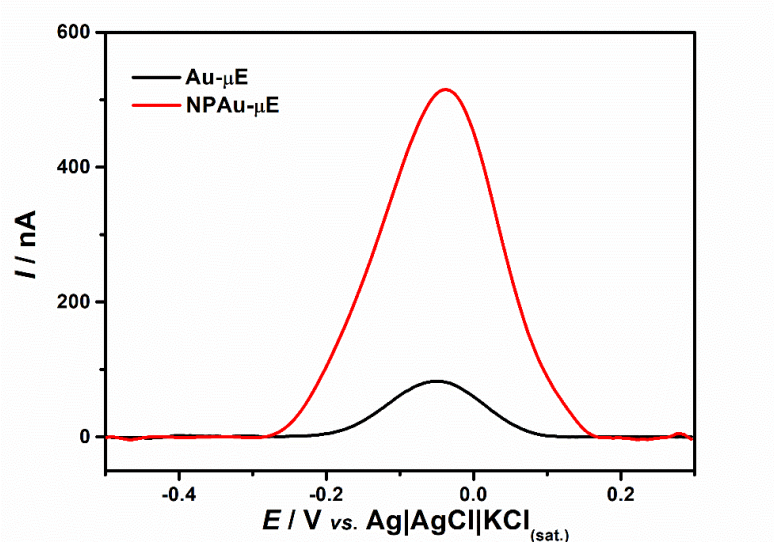

Figure 6. Electrochemical response by SWASV for 50 µg L^{-1} Pb^{2+} using NPAu-µE (red line) and Au-µE (black line). Supporting electrolyte: 0.10 mol L^{-1} acetate buffer (pH = 4.5). SWASV conditions: f = 25 Hz; ΔE = 5 mV; a = 50 mV; $R_{stirring}$ = 2000 rpm; deposition time = 120 s, deposition potential = -0.5 V.

Next, calibration curves were prepared with increasing Pb^{2+} concentrations (40.0 to 110.0 µg L^{-1}) using the optimized conditions of SWASV (Table S3) and a good linearity was obtained (R = 0.998, see Figure 7). LOD and LOQ values were calculated in 5.0 and 15.0 µg L^{-1}, respectively. An adequate precision of the electrochemical measurements was verified (RSD = 4.3%) through a repeatability study (n = 10). In order to demonstrate the potential application of the method, spiked tap water sample (corresponding to 50.0 µg L^{-1} Pb^{2+} in electrochemical cell) was analyzed, and recovery percentage of 85±2 % was achieved, indicating a good accuracy of the method.

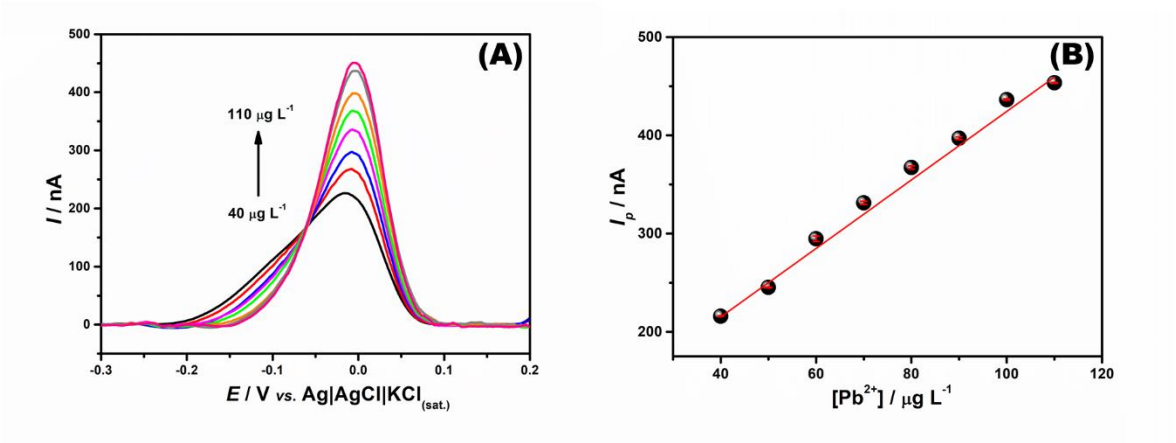

Figure 7. (A) baseline-corrected SWASV scans obtained for increasing concentrations of lead (II) (40.0 – 110.0 μg L^{-1}) in supporting electrolyte 0.10 mol L^{-1} acetate buffer (pH = 4.5) and **(B)** Respective calibration curve. SWASV conditions are described in Table S3.

This preliminary result indicates the feasibility of the proposed sensor for metal determination. Table S4 showed the comparison between the analytical performance of the NPAu-μE sensor for the detection of Pb^{2+} with other electrochemical sensors. As can be seen, although the proposed sensor has a higher LOD, a wide linear range under a lower deposition time was established. Furthermore, opposite to other sensors that use toxic metals for surface modification, this sensor requires only a simple electrochemical treatment in acid medium to improve the analytical response.

Conclusion

In this work, it was demonstrated that a disposable gold microelectrode array can be used as an efficient electrochemical sensor after a simple and eco-friendly surface treatment. This treatment provided more exposure of active sites, which improved the electrochemical response of inorganic and organic species. The potential application of the proposed sensor was investigated for the determination of DIP by BIA-AD and Pb^{2+} by SWASV. In both cases, analytical performances comparable to other more expensive

electrochemical sensors were obtained. Therefore, the developed sensor proves to be a viable and promising analytical tool for quality control of pharmaceutical formulations, as well as monitoring of metals in environmental samples.

Acknowledgments

The authors are grateful for the financial support provided by Brazilian funding agencies: the Foundation for the Support of Research, Scientific and Technological Development of Maranhão – FAPEMA (Grant number: INFRA-02263/21; UNIVERSAL-01372/17); National Council for Scientific and Technological Development – CNPq (307271/2017-0 and 163330/2020-4); Coordination of Superior Level Staff Improvement - CAPES (Project SCBA 88887.472618/2019-00, Finance Code 001); and INCTBio (CNPq grant no. 465389/2014–7).

References

1. X. J. Huang, A. M. O'Mahony, and R. G. Compton, *Small*, **5**, 776–788 (2009).

2. T. J. Davies and R. G. Compton, *J. Electroanal. Chem.*, **585**, 63–82 (2005).

3. A. Di Credico, G. Gaggi, P. Izzicupo, L. Ferri, L. Bonanni, G. Iannetti, A. Di Baldassarre, and B. Ghinassi, *Biosensors*, **11**, 450 (2021).

4. C. Y. Lee, Y. J. Tan, and A. M. Bond, *Anal. Chem.*, **80**, 3873–3881 (2008).

5. K. Nishio and H. Masuda, *Angew. Chemie Int. Ed.*, **50**, 1603–1607 (2011).

6. M. L. Chelaghmia, M. Nacef, A. M. Affoune, M. Pontié, and T. Derabla, *Electroanalysis*, **30**, 1117–1124 (2018).

7. M. Lou Tercier-Waeber, M. Fighera, M. Abdou, E. Bakker, and P. van der Wal, *Sensors Actuators, B Chem.*, **328**, 128996 (2021).

8. H. Jeong and J. Kim, *Appl. Surf. Sci.*, **297**, 84–88 (2014).

9. R. Zeis, T. Lei, K. Sieradzki, J. Snyder, and J. Erlebacher, *J. Catal.*, **253**, 132–138 (2008).

10. K. Rong, L. Huang, H. Zhang, J. Zhai, Y. Fang, and S. Dong, *Chem. Commun.*, **54**, 8853–8856 (2018).

11. J. Jia, L. Cao, and Z. Wang, *Langmuir*, **24**, 5932–5936 (2008).

12. A. Sukeri, L. P. H. Saravia, and M. Bertotti, *Phys. Chem. Chem. Phys.*, **17**, 28510–28514 (2015).

13. D. X. O. Jaramillo, A. Sukeri, L. P. H. Saravia, P. J. Espinoza-Montero, and M. Bertotti, *Electroanalysis*, **29**, 2316–2322 (2017).

14. A. E. B. Lima, G. E. Lima, E. Longo, L. S. Cavalcanti, and R. S. Santos, *Electroanalysis*, **28**, 985–989 (2016).

15. M. A. Augelli, V. B. Nascimento, J. J. Pedrotti, I. G. R. Gutz, and L. Angnes, *Analyst*, **122**, 843–847 (1997).

16. B. D. Pacheco, J. Valério, L. Angnes, and J. J. Pedrotti, *Anal. Chim. Acta*, **696**, 53–58 (2011).

17. G. Higino, Í. Machado, G. Nascimento, and J. Pedrotti, *J. Braz. Chem. Soc.*, **32**, 2215–2221 (2021).

18. D. P. Rocha, A. L. Squissato, S. M. da Silva, E. M. Richter, and R. A. A. Munoz, *Electrochim. Acta*, **335**, 1–11 (2020).

19. H. Wan, Q. Sun, H. Li, F. Sun, N. Hu, and P. Wang *Sensors Actuators B Chem.*, **209**, 336–342 (2015).

20. R. M. Cardoso, D. M. H. Mendonça, W. P. Silva, M. N. T. Silva, E. Nossol, R. A. B. da Silva, E. M. Richter, and R. A. A. Munoz, *Anal. Chim. Acta*, **1033**, 49–57 (2018).

21. X. Zong, R. Zhu, and X. Guo, *Sci. Rep.*, **5**, 1–10 (2015).

22. L. P. Hernández-Saravia, A. Sukeri, and M. Bertotti, *Int. J. Hydrogen Energy*, **44**, 15001–15008 (2019).

23. R. A. A. Muñoz, R. C. Matos, and L. Angnes, *J. Pharm. Sci.*, **90**, 1972–1977 (2001).

24. R. P. Bacil, R. M. Buoro, R. P. Da-Silva, D. B. Medinas, A. W. Lima, and S. H. Serrano *ECS Trans.*, **43**, 251–258 (2019).

25. D. P. Rocha, R. M. Cardoso, T. F. Tormin, W. R. de Araujo, R. A. A. Munoz, E. M. Richter, and L. Angnes, *Electroanalysis*, **30**, 1386–1399 (2018).

ARTIGO / Supplementary material

Supplementary material

Nanoporous gold microelectrodes arrays using microchips: A highly sensitive and cost-effective platform for electroanalytical applications

Gilvana Pereira Siqueira[a], Lucas Vinícius de Faria[b], Raquel Gomes Rocha[b], Eduardo Mathias Richter[b], Rodrigo Alejandro Abarza Muñoz[b], Iranaldo Santos da Silva[c], Luiza Maria Ferreira Dantas[c**].*

[a]*Departamento de Química, Centro de Ciências Exatas e Tecnologia, Universidade Federal do Maranhão, 65080-805, São Luís, MA, Brasil;*

[b]*Instituto de Química, Universidade Federal de Uberlândia, 38400-902, Uberlândia, Minas Gerais, Brasil;*

[c]*Departamento de Tecnologia Química, Centro de Ciências Exatas e Tecnologia, Universidade Federal do Maranhão, 65080-805, São Luís, MA, Brasil;*

Corresponding author:

[*]*munoz@ufu.br* *ORCID: 0000-0001-8230-5825*

[**]*luiza.dantas@ufma.br* *ORCID: 0000-0002-2805-9253*

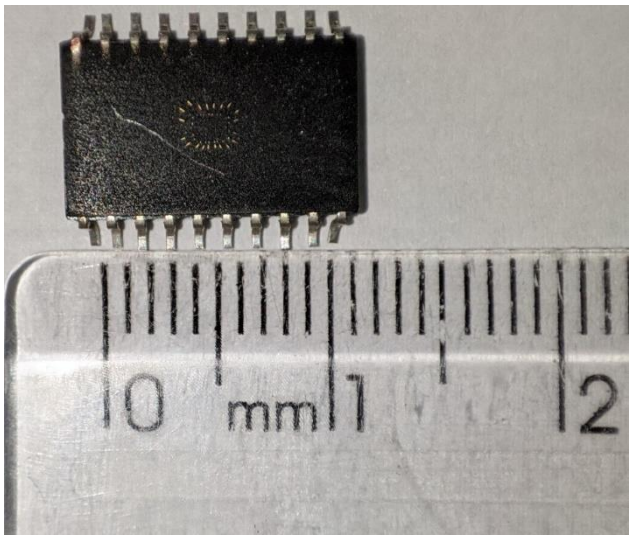

Figure S1. Real image of SMD device used as working electrode.

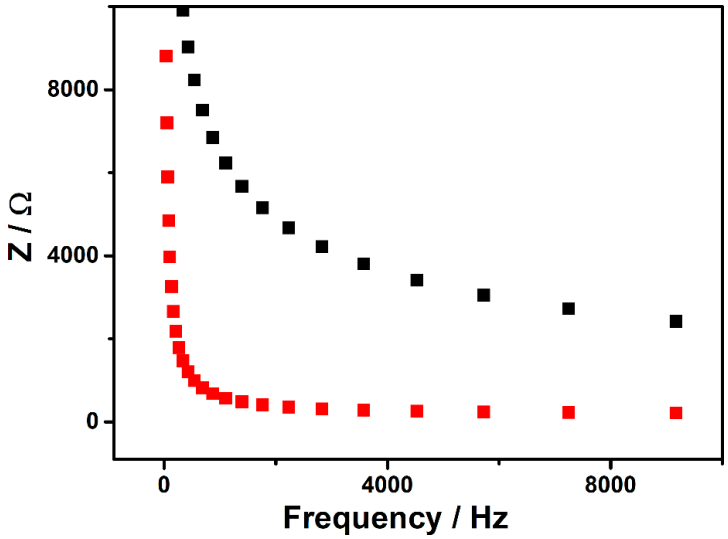

Figure S2. Impedance measurement results (Bode plots) using 10.0 mmol L^{-1} ferricyanide potassium in the presence of 1.0 mol L^{-1} KCl for Au-µE (black line) and NPAu-µE (red line).

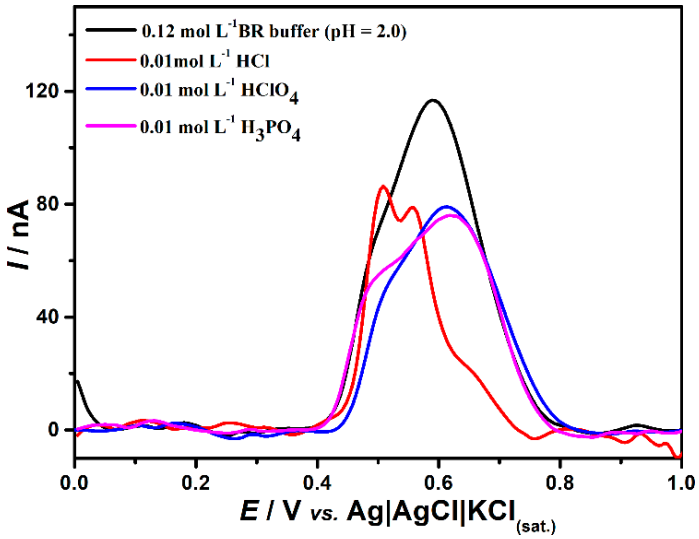

Figure S3. Baseline-LSV response for 0.50 mmol L^{-1} DIP in different supporting electrolytes, using NPAu-µE electrode. LSV conditions: Scan rate: 50 mV s^{-1}; step potential: 5 mV.

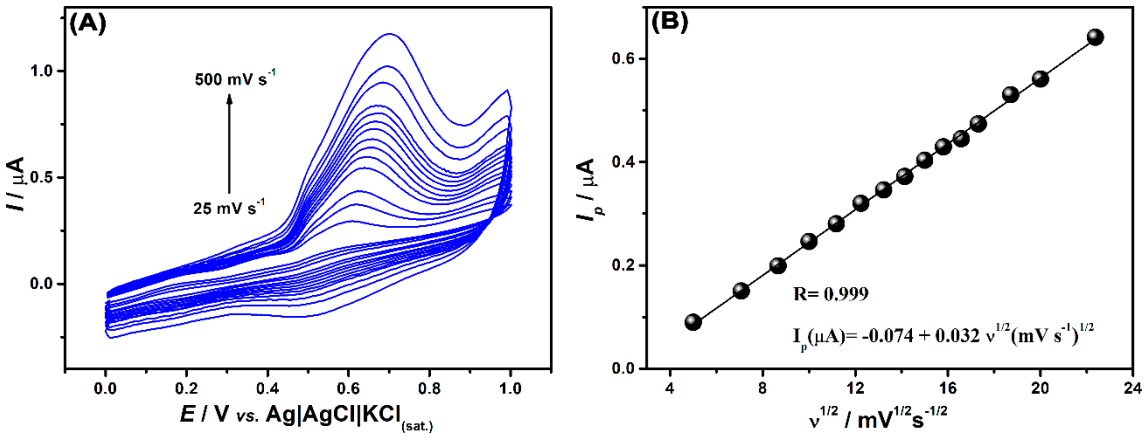

Figure S4. (A) Cyclic voltammetric response of 0.50 mmol L^{-1} DIP in 0.12 mol L^{-1} BR buffer (pH = 2.0) in different scan rate (25 to 500 mV s^{-1}) using NPAu-µE as working electrode, and **(B)** linear relationship between peak current (I_p) and square root of the scan rate ($v^{1/2}$).

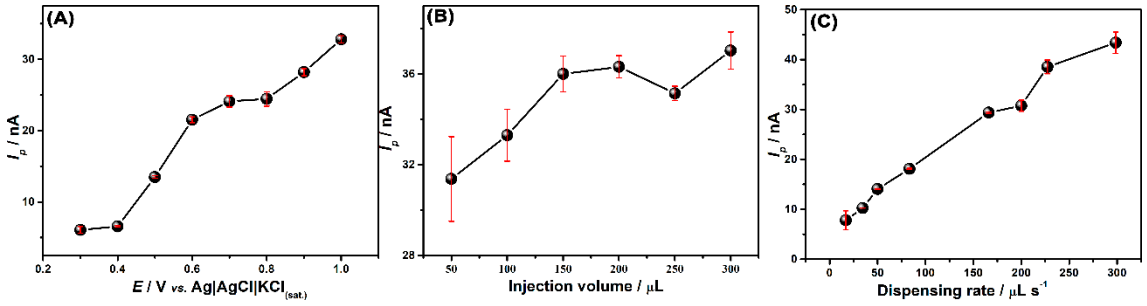

Figure S5. (A) Hydrodynamic voltammograms obtained with the BIA-AD by plotting the peak current values as function of the corresponding analysis potential using NPAu-µE as working electrode; Effect of dispensing rate **(B)** and injection volume **(C)** on the amperometric response of 50.0 µmol L^{-1} DIP. Supporting electrolyte: 0.12 mol L^{-1} BR buffer (pH = 2.0).

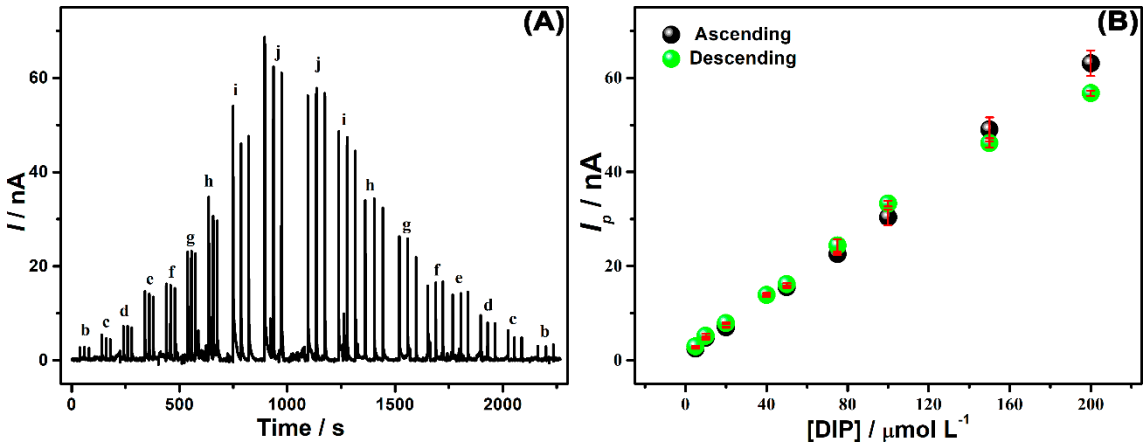

Figure S6. (A) Baseline-corrected amperograms of successive injections (n = 3) of DIP standard solution (b-j: 5.0 to 200.0 µmol L^{-1}) in increasing and decreasing concentrations, using the Au-µE as working electrode, and **(B)** Respective calibration curves of DIP. BIA-AD conditions: Applied potential = +0.7 V; supporting electrolyte: 0.12 mol L^{-1} BR buffer (pH = 2.0); V_{inj} = 200 µL, R_{dis} = 227.3 µL s^{-1}.

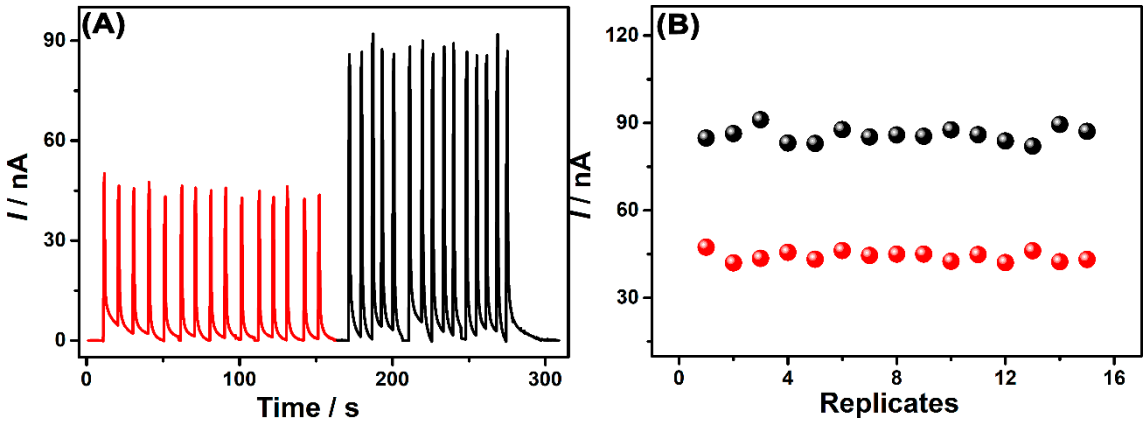

Figure S7. (A) Baseline-corrected amperograms obtained from successive injections (n = 15) of 50.0 µmol L^{-1} (red line) and 100.0 µmol L^{-1} (black line) DIP; **(B)** Respective variation of current intensities. BIA-AD conditions: Applied potential = +0.7 V; supporting electrolyte: 0.12 mol L^{-1} BR buffer (pH 2.0); V_{inj} = 200 µL, R_{dis} = 227.3 µL s^{-1}.

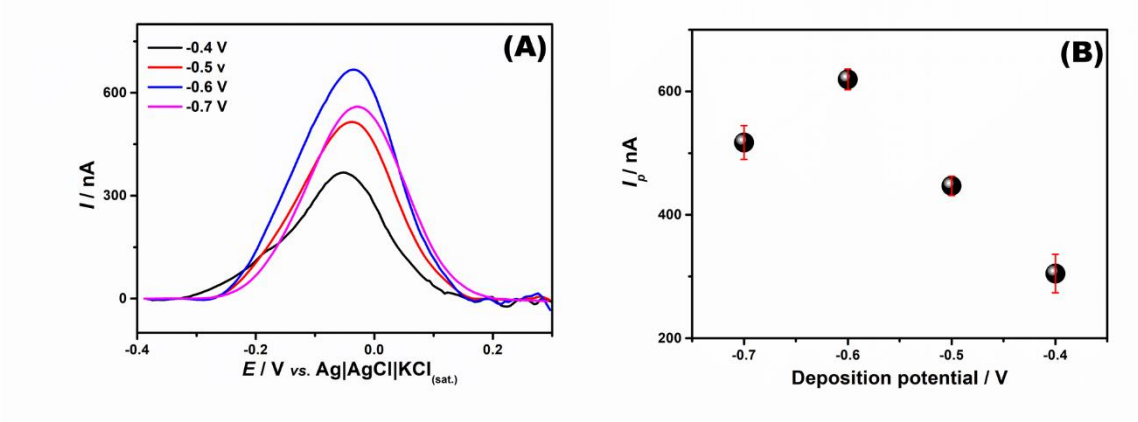

Figure S8. (A) Baseline corrected SWASV to evaluate the effect of deposition potential (-0.4 V to -0.7 V) on the peak current of 50.0 µg L^{-1} Pb^{2+} and **(B)** the respective peak current for each studied parameter value. Working electrode: NPAu-µE. Supporting electrolyte: 0.1 mol L^{-1} acetate buffer (pH = 4.5). SWASV conditions: f = 25 Hz; ΔE = 5 mV; a = 50 mV; stirring rate= 2000 rpm; deposition time = 120 s.

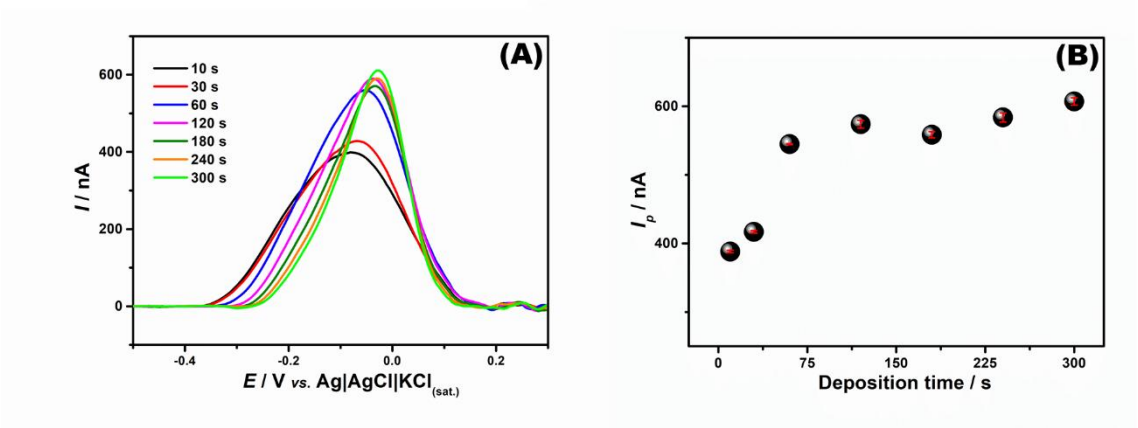

Figure S9. **(A)** Baseline corrected SWASV to evaluate the effect of deposition time (10-300 s) on the peak current of 50.0 µg L^{-1} Pb^{2+} and **(B)** the respective peak current for each studied parameter value. Working electrode: NPAu-µE. Supporting electrolyte: 0.10 mol L^{-1} acetate buffer (pH = 4.5). SWASV conditions: *f* = 25 Hz; ΔE = 5 mV; *a* = 50 mV; stirring rate = 2000 rpm; deposition potential = -0.6 V.

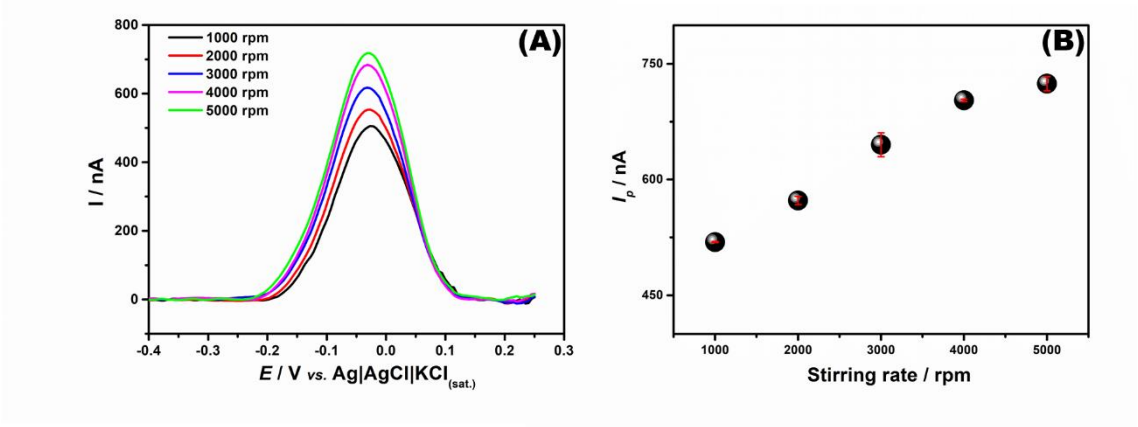

Figure S10. (A) Baseline corrected SWASV to evaluate the effect of stirring rate (1000-5000 rpm) on the peak current of 50.0 µg L^{-1} Pb^{2+} and **(B)** the respective peak current for each studied parameter value. Working electrode: NPAu-µE. Supporting electrolyte: 0.10 mol L^{-1} acetate buffer (pH = 4.5). SWASV conditions: *f* = 25 Hz; ΔE = 5 mV; *a* = 50 mV; deposition time = 60 s; deposition potential = -0.6 V.

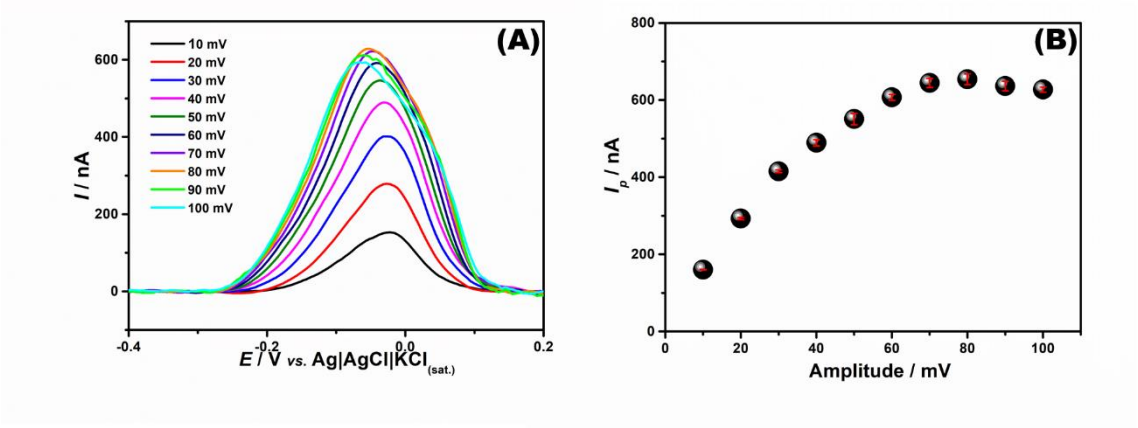

Figure S11. (A) Baseline corrected SWASV to evaluate the effect of amplitude (10-100 mV) on the peak current of 50.0 µg L^{-1} Pb^{2+} and **(B)** the respective peak current for each studied parameter value. Working electrode: NPAu-µE. Supporting electrolyte: 0.10 mol L^{-1} acetate buffer (pH = 4.5). SWASV conditions: f = 25 Hz; ΔE = 5 mV; deposition time = 60 s; deposition potential = -0.6 V; stirring rate = 4000 rpm.

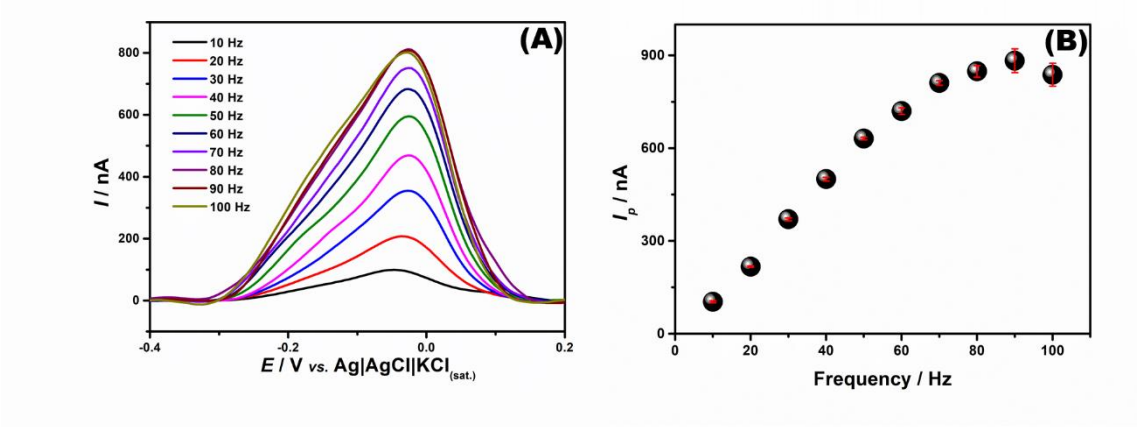

Figure S12. (A) Baseline corrected SWASV to evaluate the effect of frequency (10-100 Hz) on the peak current of 50.0 µg L^{-1} Pb^{2+} and **(B)** the respective peak current for each studied parameter value. Working electrode: NPAu-µE. Supporting electrolyte: 0.10 mol L^{-1} acetate buffer (pH = 4.5). SWASV conditions: a = 30 mV; ΔE = 5 mV; deposition time= 60 s; deposition potential = -0.6 V; stirring rate = 4000 rpm.

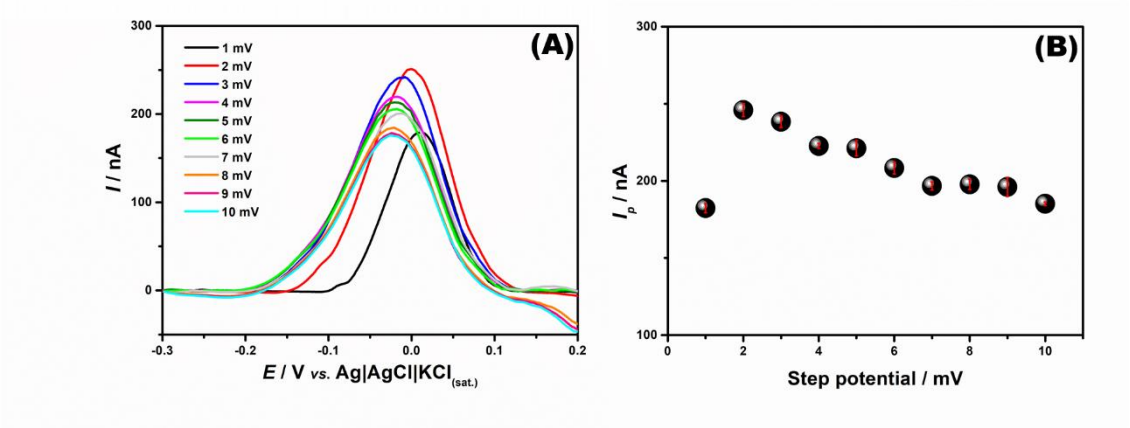

Figure S13. (A) Baseline corrected SWASV to evaluate the effect of step potential (1-10 mV) on the peak current of 50.0 µg L^{-1} Pb^{2+} and **(B)** the respective peak current for each studied parameter value. Working electrode: NPAu-µE. Supporting electrolyte: 0.10 mol L^{-1} acetate buffer (pH = 4.5). SWASV conditions: f = 30 Hz; a = 30 mV; deposition time = 60 s; deposition potential = -0.6 V; stirring rate = 4000 rpm

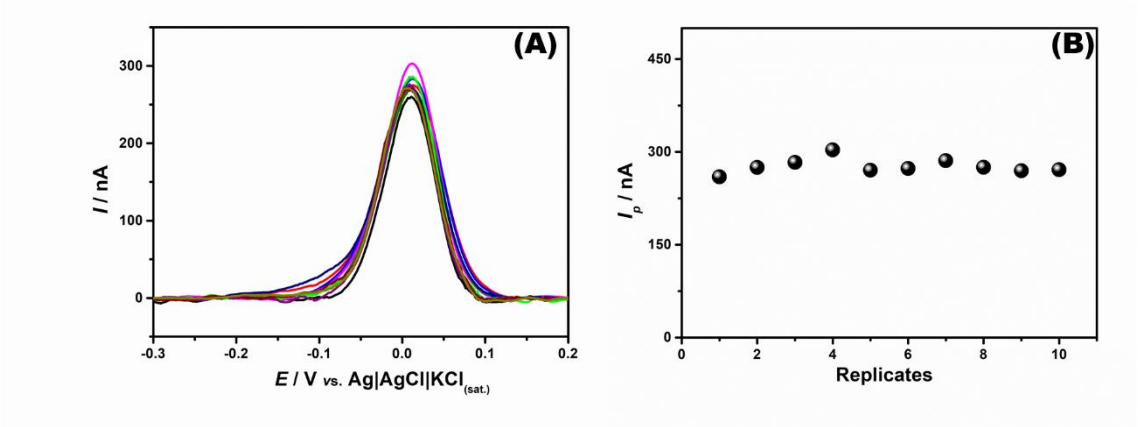

Figure S14. SWASV baseline-corrected obtained from successive measurements (n = 10) of 60.0 µg L^{-1} Pb^{2+}; **(B)** Respective variation of current intensities. SWASV conditions are described in Table S3.

Table S1. Studied range and selected optimized values for the determination of DIP using BIA-AD.

Parameters	Studied range	Optimized value
Potential / V (*vs.* Ag|AgCl|KCl$_{(sat.)}$)	0.3 – 1.0	+0.7
Dispensing rate / µL s^{-1}	16.9-298.5	227
Injection volume / µL	50-300	200

Table S2. Comparison of the developed method with other electroanalytical methods reported in the literature for DIP detection.

Electrode	Method	Linear range / µmol L^{-1}	LOD / µmol L^{-1}	Ref.
Nickel-salen/Pt	AMP	4.7 – 110	1.20	[1]
CD-HPC/CPCE	SWV	0.5 – 35	0.009	[2]
PTH/MWCNT/ CFE	DPV	250 – 2500	13.4	[3]
RF/GCE	SWV	0.1 – 2.7	0.10	[4]
CrGO/GCE	AMP	48 – 246	0.13	[5]
CDGE	FIA-AD	1 – 10	0.10	[6]
GCE	SWV	10 – 100	3.00	[7]
NPAu-µE	BIA-AD	1 – 200	0.57	**This work**

Nickel Salen/Pt: (Salen = N,N-ethylenebis(salicydeneiminato) film coated platinum electrode; CD-HPC/CPCE: Carbon black paste electrode modified with α-cyclodextrin and hierarchical porous carbon; PTH/MWCNT/CFE: Multi-walled carbon nanotube-poly(thionine) nanostructures formed on carbon film electrodes ; RF/GCE: Nano riboflavine modified glassy carbon electrode; CrGO/GCE: Chemically-reduced graphene-oxide modified glassy carbon electrode; CDGE: Compact disc gold electrode; GCE: Glassy carbon electrode; NPAu-µE: Nanoporous gold microelectrode array; AMP: Amperometry; SWV: Square wave voltammetry; DPV: Differential pulse voltammetry; FIA-AD: Flow injection analysis with amperometric detection; BIA-AD: Batch injection analysis with amperometric detection.

Table S3. Studied ranges and selected optimized values for the determination of lead (II) using SWASV.

Parameters	Studied range	Optimized value
Frequency/ Hz	10 - 100	30
Step potential / mV	1 - 10	2
Amplitude / mV	10 - 100	30
Deposition potential / V	-0.4 / -0.7	-0.6
Deposition time/ s	10 - 300	60
Stirring rate/ rpm	1000 - 5000	4000

Table S4. Comparison of the proposed sensor with other electrochemical sensors reported in the literature for Pb^{2+} determination.

Electrode	Method	Deposition time / s	Linear range / µg L^{-1}	LOD / µg L^{-1}	Ref.
MF/GCE	SWASV	240	10 – 46	0.9	[8]
HMDE	AdSV	160	0.5 - 70	0.02	[9]
BiFE	SWASV	600	0.02- 0.40	0.005	[10]
SPE/AuF	SWASV	120	4 – 16	0.5	[11]
SPGE/GNPs	SWASV	120	20 – 200	2.0	[12]
SbNP/MWCNT/CPE	SWASV	120	10 – 60	0.65	[13]
PolyL/GCE	DPASV	60	0.2 – 20	0.15	[14]
NPAu-µE	SWASV	60	40 – 110	5.0	**This work**

MF/GCE: Glassy carbon electrode modified with mercury-film; HMDE: hanging mercury drop electrode; BiFE: Bismuth film electrode; SPE/AuF: Screen-printed electrodes modified with gold films SPGE/GNPs screen-printed gold electrode modified with gold nanoparticles; SbNP/MWCNT/CPE: Antimony nanoparticle-multiwalled carbon nanotubes composite immobilized at carbon paste electrode; PolyL/GCE: Glassy carbon electrode with poly(4-azulen-1-yl-2,6-bis(2-thienyl)pyridine); SWASV: Square wave anodic stripping voltammetry; AdSV: Adsorptive stripping voltammetry; DPASV: Differential pulse anodic stripping voltammetry.

References

1. M. F. S. Teixeira and T. R. L. Dadamos, *Procedia Chem.*, **1**, 297–300 (2009).

2. A. Wong, A. C. Riojas, A. M. Baena-Moncada, and M. D. P. T. Sotomayor, *Microchem. J.*, **164**, 106032 (2021).

3. M. E. Ghica, G. M. Ferreira, and C. M. A. Brett, *J. Solid State Electrochem.*, **19**, 2869–2881 (2015).

4. G. Gopu, P. Manisankar, B. Muralidharan, and C. Vedhi, *Int. J. Electrochem.*, **2011** (2011).

5. L. V. de Faria, T. P. Lisboa, G. C. Azevedo, R. A. Sousa, M. A. C. Matos, R. A. A. Munoz, R. C. Matos, *Electroanalysis*, **31**, 646–651 (2019).

6. R. A. A. Muñoz, R. C. Matos, and L. Angnes, *J. Pharm. Sci.*, **90**, 1972–1977 (2001).

7. R. P. Bacil, R. M. Buoro, O. S. Campos, M. A. Ramos, C. G. Sanz, and S. H. P. Serrano, *Electrochim. Acta*, **273**, 358–366 (2018).

8. T. P. Lisboa, L. V. de Faria, M. A. C. Matos, R. C. Matos, and R. A. de Sousa, *Microchem. J.*, **150**, 104183 (2019).

9. S. Abbasi, K. Khodarahmiyan, and F. Abbasi, *Food Chem.*, **128**, 254–257 (2011).

10. I. Gęca and M. Korolczuk, *Talanta*, **171**, 321–326 (2017).

11. A. Mandil, L. Idrissi, and A. Amine, *Microchim. Acta*, **170**, 299–305 (2010).

12. H. Wan, Q. Sun, H. Li, F. Sun, N. Hu, and P. Wang *Sensors Actuators B Chem.*, **209**, 336–342 (2015).

13. A. M. Ashrafi, S. Cerovac, S. Mudric, V. Guzsvany, L. Husakova, I. Urbanova, and K. Vytras, *Sensors Actuators B Chem.*, **191**, 320–325 (2014).

14. G.-O. Buica, E.-M. Ungureanu, L. Birzan, A. C. Razus, and L.-R. Mandoc (Popescu), *J. Electroanal. Chem.*, **693**, 67–72 (2013).